2021

Application of a Color Change Coating to Evaluate Flow Velocity Distribution and Wall Shear Stress of Fan Blade

Min Che
University of Illinois Urbana-Champaign, minche2@illinois.edu

Stefan Elbel

Application of a Color Change Coating to Evaluate Flow Velocity Distribution and Wall Shear Stress of Fan Blade

Min CHE[(a)], Stefan ELBEL[(a,b,*)]
[(a)] Air Conditioning and Refrigeration Center,
Department of Mechanical Science and Engineering,
University of Illinois at Urbana-Champaign,
1206 West Green Street, Urbana, IL 61801, USA
[(b)] Creative Thermal Solutions, Inc.,
2209 North Willow Road, Urbana, IL 61802, USA
[(*)] Corresponding Author
Email: elbel@illinois.edu

ABSTRACT

A mass transfer method has been employed to characterize tangential flow velocity around fan blades. In the current research, two commercial air-conditioning fan blade samples have been investigated. The blade surfaces were covered with a 10 μm yellow coating by a spray method. The fan and a camera are driven by a motor and shaft system that can synchronize the rotational speed. Therefore, a relative stay still image of the fan blade during rotation can be obtained. Subsequently, a small amount (50 ppm_v) of ammonia has been injected into an environmental chamber that has the fan installed and rotating. The coating material on the blade surfaces absorbs the ammonia from the airflow and responds with a color change from yellow to blue. At the same time, the color change was recorded by the camera. The surface color change can be quantified by image processing which represents the local mass transfer. According to the fluid mechanics and analogy between mass transfer, heat transfer, and Colburn's relation for turbulent flow, local tangential flow velocity distribution at the external of the boundary layer on the blade surface can be quantified. Thereafter, friction factor and wall shear stress can be calculated accordingly. Comparing to other experimental and computational methods, this new experimental method provides a robust way to evaluate turbulent flow velocity around the rotational fan blades. The results show this method is promising to be employed to evaluate and optimize fan systems to improve efficiency and reduce noise.

1. INTRODUCTION

The mechanical means of moving air for industrial and cooling purposes have been realized for many centuries. Axial flow fan moves air or gas parallel to the axis of rotation. This type of fan has been widely applied for low pressure resistance and high flow rate applications such as ventilation, the outdoor unit of air-conditioning, and cooling for electronic devices. The main principle of an axial fan design is to fulfill a specific volumetric flow rate and static pressure requirements in a constrained space and at the same time maximum reliability and minimum energy consumption and noise. Therefore, many parameters need to be manipulated such as blade size, blade shape, shroud geometry, hub structure, motor mounting, installation frame, and air duct. The fan blade is the main component that is attached to the rotor and delivering work to the fluid. Therefore, investigation of the interaction between the fan blade and its surrounding air is crucial. Tip leakage, trailing edge vortex, hub vortex, end wall vortex between shroud and blade tip, profile losses due to turbulent boundary layer on blade surface have been recognized as the sources of main losses in axial fan applications. Fukano *et al*. (1977) have experimentally investigated the relationship between fan blade parameters and noise. They have measured axial fans with various blade shapes in a wind tunnel and made a comparison of noise values. They have evaluated the total power, flow rate, and sound level by adjusting chord length, stagger angle, number of blades, rotation speed, and trailing edge thickness. Two most effective approaches have been proposed to reduce noise: thinning the blade thickness at the trailing edge and optimizing the shape of the blade sweep. However, without the fluid field measurement, the mechanism of the better design cannot be visualized or be proved.

The instability of fluid, not only cause energy losses but also generate unpleasant noise. According to Wallis (1961), the sources of fan noise include periodic pressure fields created by the rotor blades; vortex noise associated with the

turbulence present in shear flows; and mechanical vibrations which may or may not be aerodynamically excited. In conclusion, a steady flow field surrounding the rotor blades is expected in order to minimize the noise and improve fan efficiency. In recent years, some technology such as Particle Image Velocimetry (PIV) can be used to obtain flow velocity field. However, it is challenging to measure the rotational fan blades and the experimental setup is usually complex and costly. Therefore, CFD simulation is often employed to visualize the distribution of velocity field and explain the mechanism of a better fan blade design. Yang *et al*. (2007) have proposed a circumferential forward-skewed blade shape based on a 3D Navier-Stokes (N-S) flow solver of CFD. They have experimentally verified that the new design has increased the efficiency by 1.27%, and reduced noise by 6 dB(A). The flow velocity distributions of the initial impeller and the optimized impeller have been compared from the model. The optimized impeller shows a reduced aerodynamic loss near the region of the blade shroud and hub end wall. Jung and Joo (2019) have employed CFD solver SC/Tetra to investigate the pressure loss of a three-blade air-conditioning axial fan. The results show that tip vortex and shroud wall losses take up 69.7% of the total loss, the blade profile loss accounts for 11.8%, and the hub loss accounts for 18.5%. The experiment of local flow velocity has been conducted by using hot-bulb-type probes to verify the model. The probes were located at the point that is 50 mm away from the fan's hub in the axial direction which cannot be closer to the blade surface due to rotation. Therefore, the obtained velocity distribution does not represent the tangential flow velocity at the boundary layer of the blade surface. Wang *et al*. (2011) also employed the CFD model to obtain boundary layer flow velocity, wall shear stress, and static pressure gradient on blade surfaces. Afterward, an empirical correlation from the fan noise experiment is applied to the integral formula to predict the noise spectrum. The comparison of sound power between CFD prediction and experimental measurements shows large differences, especially at low frequency.

The boundary layer thickness and flow structure around the blades affect the total pressure and flow rate, the wall shear stress causes loss due to friction on the blade surface. Therefore, it is essential to study these aerodynamic parameters to optimize the design of the fan system. However, existing experimental methods cannot provide the local measurements especially when the surface geometry is complex. Therefore, local results from CFD simulations cannot be verified. Incorrect assumptions may be made by only comparing the global results such as total flow rate, static pressure, and sound power. To address this issue, the CTC method proposed by Che and Elbel (2019) has been employed to evaluate local flow velocity on the surfaces of fan blades. According to Che and Elbel (2019) in Figure 1, the process involves a thin, acidic coating on the substrate surface which is exposed to a low concentration of ammonia tracer gas mixed with flowing air. The coating absorbs ammonia and water vapor and gradually changes color from yellow to blue. By observing and quantifying the color change, the local mass transfer can be obtained. Then local heat transfer can be subsequently calculated by applying the analogy between heat and mass transfer. Afterward, local Reynolds number and heat transfer can be correlated from Colburn's relation. As a result, the local tangential flow velocity is obtained. In the current research, two commercial air-conditioning fan blades have been investigated. The color change material is coated to both high-pressure and low-pressure sides of the fan blades to quantify local tangential velocity distribution at the external of the boundary layer. Comparing to previous experimental and computational methods, current research provides a robust and low-cost way to evaluate the aerodynamic characteristics of rotating fan blades.

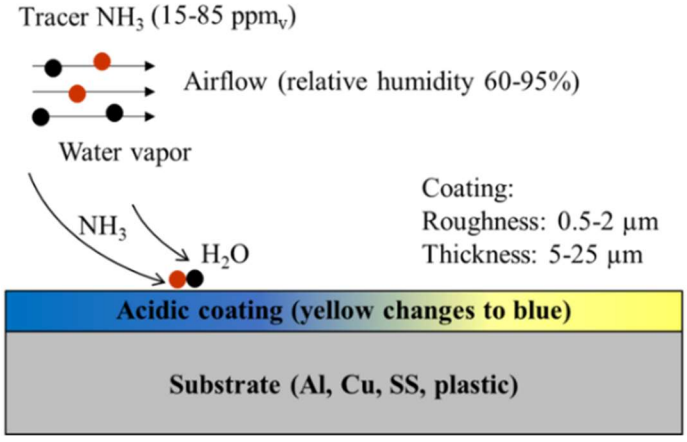

Figure 1: Principle of the CTC method by Che and Elbel (2019)

2. METHODOLOGY

2.1 Analogy between Mass Transfer, Heat Transfer, and Momentum Transfer

A schematic of the boundary layer of laminar flow over a flat plate is shown in Figure 2. The assumptions include incompressible fluid, no-slip, and an impermeable wall which are well accepted for laminar flow over a solid plate. For ammonia at a low concentration (50 ppm_v), the impermeable-surface assumption still holds. In Figure 2, the shapes of velocity, temperature, and concentration profiles are similar. For heat transfer, it shows a constant temperature difference between the wall and the free stream fluid. For mass transfer, the dilute ammonia gas is absorbed by the coating material. Therefore, the concentration of ammonia at the wall is assumed to be zero.

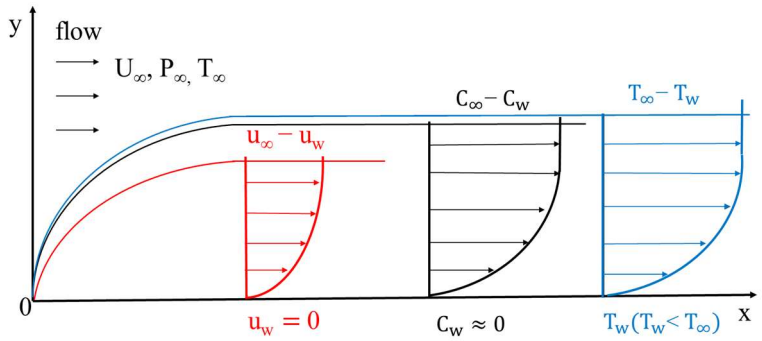

Figure 2: Boundary layer of velocity, temperature, and concentration of laminar flow over a flat plate

Due to the similarity theory and analogy between heat, mass, and momentum transfer, if one of them can be measured, others can be easily calculated. According to Bejan (1995), the analogy is also valid on turbulent flow because the format of momentum equation in the x-direction, energy equation, and concentration equation are similar as shown in Equations (1) to (3).

$$\bar{u}\frac{\partial \bar{u}}{\partial x} + \bar{v}\frac{\partial \bar{u}}{\partial y} = \frac{\partial}{\partial y}\left[(\nu + \epsilon_M)\frac{\partial \bar{u}}{\partial y}\right] \tag{1}$$

$$\bar{u}\frac{\partial \bar{T}}{\partial x} + \bar{v}\frac{\partial \bar{T}}{\partial y} = \frac{\partial}{\partial y}\left[(\alpha + \epsilon_H)\frac{\partial \bar{T}}{\partial y}\right] \tag{2}$$

$$\bar{u}\frac{\partial \bar{C}}{\partial x} + \bar{v}\frac{\partial \bar{C}}{\partial y} = \frac{\partial}{\partial y}\left[(D + \epsilon_m)\frac{\partial \bar{C}}{\partial y}\right] \tag{3}$$

For the fan system, intake flow velocity (U_i) is usually used as U_∞ and chord length (L_c) of the blade is the

shown in Equation (4) to (6).

$$\tau_w = \mu\left(\frac{\partial u_\tau}{\partial y}\right)_{y=0} \tag{4}$$

$$c_f = \frac{\tau_w}{1/2\rho {U_i}^2} \tag{5}$$

$$Re = \frac{u_\tau \cdot L_c}{\nu} \tag{6}$$

Stanton number is used to report dimensionless heat and mass transfer in the turbulent flow. Equations (7) and (8) are the empirical formula suggested by Colburn. As a result, the heat transfer Stanton number is approximately equal to the mass transfer Stanton number as shown in Equation (9) for air and ammonia mixture at 50 ppm_v, 26°C, 60% relative humidity (RH) at 101 kPa. The relations between local wall shear stress, friction factor, and Reynolds number are shown in Equations (10) and (11). Therefore, by measuring the local mass transfer coefficient, local tangential velocity and friction factor can be obtained. If the intake flow velocity is measured, local wall shear stress is determined.

$$St = 0.0296 \cdot Pr^{-2/3} Re^{-1/5} \tag{7}$$

$$St_m = 0.0296 \cdot Sc^{-2/3} Re^{-1/5} \tag{8}$$

$$\frac{St}{St_m} = \left(\frac{Pr}{Sc}\right)^{-2/3} = \left(\frac{0.74}{0.75}\right)^{-2/3} \approx 1.00 \tag{9}$$

$$St = \frac{Nu}{Re \cdot Pr} = \frac{1}{2} c_f \cdot Pr^{-2/3} \tag{10}$$

$$\frac{1}{2} c_f = \frac{\tau_w}{\rho U_i^{\,2}} = 0.0296 \cdot Re^{-1/5} \tag{11}$$

2.2 Procedure to Obtain Local Velocity

Che and Elbel (2019) have developed an image processing algorithm using MATLAB R2018a to quantify the local color change. The procedure to obtain local tangential velocity($u_{\tau loc}$) at the external of the boundary layer of fluid on the blade surface is outlined in Figure 3. Hue value is used to quantify the color of the coating before (yellow) and after (blue) the chemical reaction takes place. In Equation (12), the local tangential velocity is proportional to the rate of color change (ϵ/t), parameters in parentheses are all constants. Here M_{max}/A_{tot} is the ammonia absorption capability per unit surface area which can be determined from the mass of the coating material, the surface area, and chemical relation between the coating material and the ammonia gas; S is the color change factor (S) which is obtained by calibration; ν is the viscosity of the fluid; D is the diffusion coefficient of ammonia-in-air; ΔC is the concentration difference between the free stream and the wall.

$$u_{\tau loc}{}^{4/5} = \left(\frac{S \cdot M_{max} \cdot L_c{}^{1/5} \cdot \nu^{4/5}}{0.0296 A_{tot} \cdot \Delta C \cdot D \cdot Pr^{1/3}}\right) \cdot \frac{\epsilon}{t} \tag{12}$$

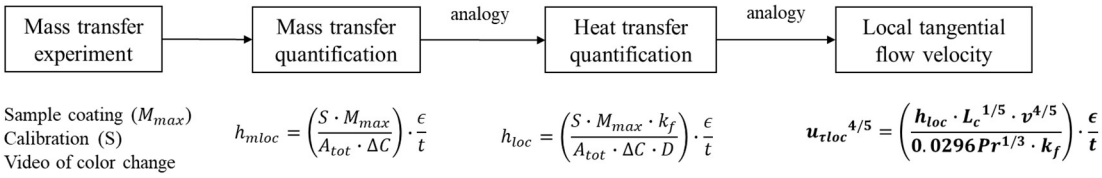

Figure 3: Procedure to obtain two-dimensional tangential flow velocity distribution [Che and Elbel (2021)]

3. EXPERIMENTAL SETUP AND PROCEDURE

3.1 Experimental Setup

As shown in Figure 4, the fan and camera are installed in a wind tunnel and are located in an environmental chamber. In the wind tunnel, the shafts of the fan blade and the camera are connected through the belt system to make sure the camera and the fan are rotating at the same speed. The rotating speed of the motor can be adjusted from 0 to 3450 RPM. The environmental chamber is employed to provide temperature, RH, and ammonia concentration control. Table 1 shows the parameters of measurements and their uncertainties.

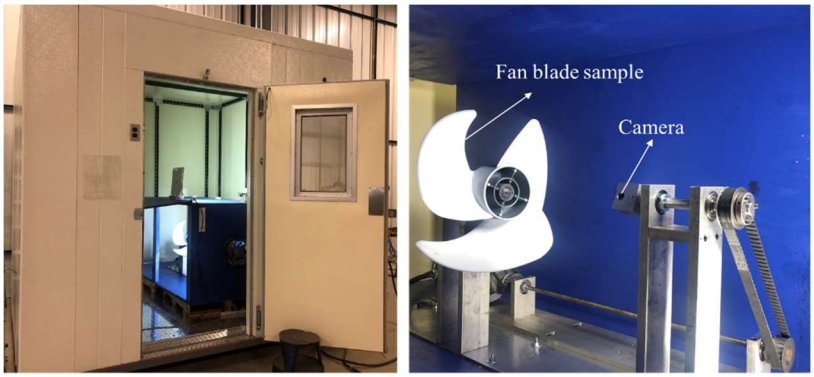

(a) The environmental chamber (b) Fan blade, camera and shaft system

Figure 4: Environmental chamber and fan blade test setup, (a) The environmental chamber, (b) Fan blade, camera, and shaft system

Table 1: Uncertainty of measurements

Parameter	Sensor	Units	Range of test	Uncertainty
Airflow temperature	Type-T thermocouples	°C	-7 to 55	± 0.3
Relative humidity (RH)	Humidity transmitter	%	0 to 100	± 5% reading
Ammonia concentration	Electrochemical	ppm_v	0 to 100	± 10% reading
Rotating speed	Laser tachometer	RPM	0 to 10000	± 1

3.2 Experimental Procedure

Two fan blades from residential air-conditioning products have been used for current research. As shown in Figure 5, the samples are painted to white color on both sides for easier color observation. After the painting is completely dried, the yellow coating material (AMS 71 manufactured by Serionix, Inc.) is sprayed to the surfaces. The quantify of the coating material is determined by the total blade surface area to make sure the thickness is about 10 μm. The same thickness of coating has been applied on a flat surface for calibration to determine the color change factor S which is 0.15 in current research. The procedure of calibration has been explained by Che and Elbel (2019). The surfaces of fan blades show a bright yellow color after been coated and dried in 60 min under room temperature as shown in Figure 5. The next step is to install the coated sample on the shaft. After the temperature and relative humidity reach the test condition and are stable, the motor has been started with a 15 Hz input frequency. The rotating speed of the fan blade is measured by a laser tachometer which is 889 RPM for both fan samples. Afterward, ammonia was injected into the chamber and at the same time, the camera started to take a video. The coated surfaces change color from yellow to blue as soon as ammonia has been introduced to the airflow. Meanwhile, the concentration of ammonia in the environmental chamber is measured by an ammonia sensor inside of the chamber. Therefore, the concentration difference (ΔC) between the airflow and the blade surface can be determined. It takes 30 to 120 seconds for all coated surfaces to completely change to a blue color depends on the concentration of ammonia, coating thickness, and rotation speed. Therefore, the experiment usually only takes several minutes. The video of the color change of the tested fan blade sample can be used to obtain tangential velocity distribution as explained in Section 2.2. The coating can be flushed away by water which makes the samples reusable.

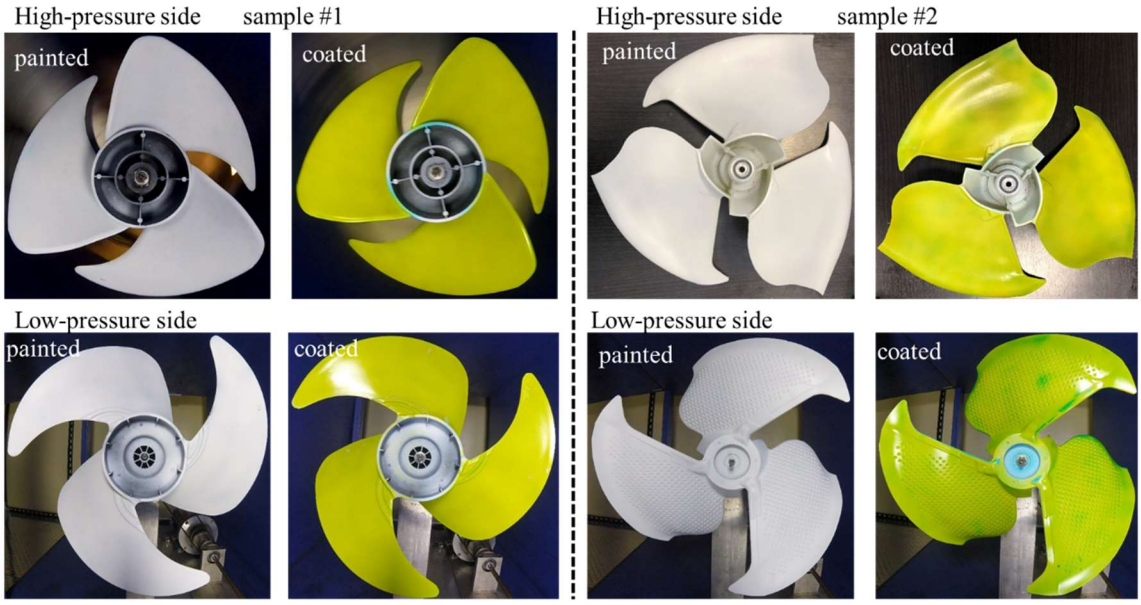

Figure 5: Fan blades sample preparation (before mass transfer experiment)

4. METHOD VALIDATION ON FUNDAMENTAL GEOMETRY

In the current study, the method accuracy has been validated on two-dimensional stagnation flow. Two-dimensional stagnation flow or Hiemenz flow is a fundamental heat transfer problem that has an analytical solution. The schematic of the Hiemenz flow is shown in Figure 6 (a) that the direction of the airflow is perpendicular to the plate surface.

According to the observation of the mass transfer experiments in the current study, the color change occurs first at the edges and then spreads towards the center of the sample. The results show higher flow velocities at the edges compared to the stagnation region at the center. Results from the current study agree with experimental results from Tien and Sparrow (1979) which employed the naphthalene sublimation method as shown in Figure 6 (b).

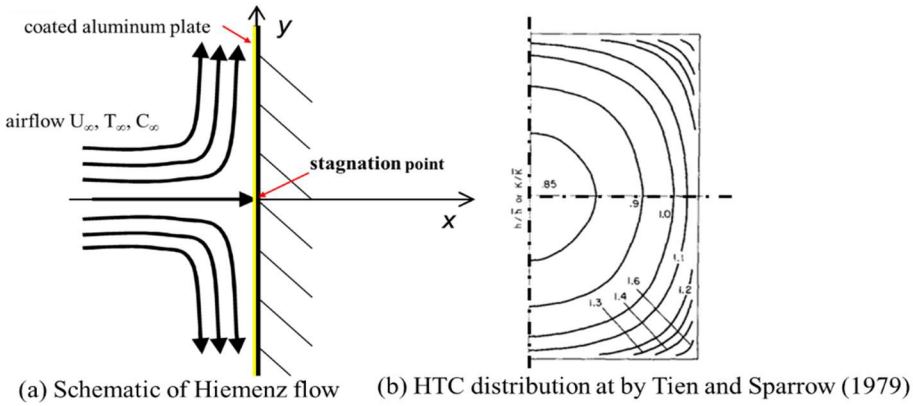

Figure 6: Hiemenz flow, (a) Schematic, (b) HTC distribution by Tien and Sparrow (1979)

Experimental results of HTC distribution (only show half-plate due to the symmetry) on an L50 x W100 mm plate in the current study are shown in Figure 7 (a). The sample was tested at 3 ms^{-1} flow velocity. The local HTCs at the edges are about 1.5 to 2 times higher than at the center location of the samples. The experimental data of local HTCs of the current research have been compared with experimental data of Ramirez *et al.* (2002). They have employed a temperature measurement method to obtain local HTCs of a narrow rectangular plate at 5ms^{-1}. As shown in Figure 7 (b), the ratio of local Nusselt numbers and averaged Nusselt numbers referring to the plate chord has been reported. Therefore, the comparison is independent of the flow velocities. The results of the current measurements agree with the results of Ramirez *et al.* (2002) within ±10% difference. Moreover, they have compared their measurements with the analytical solution.

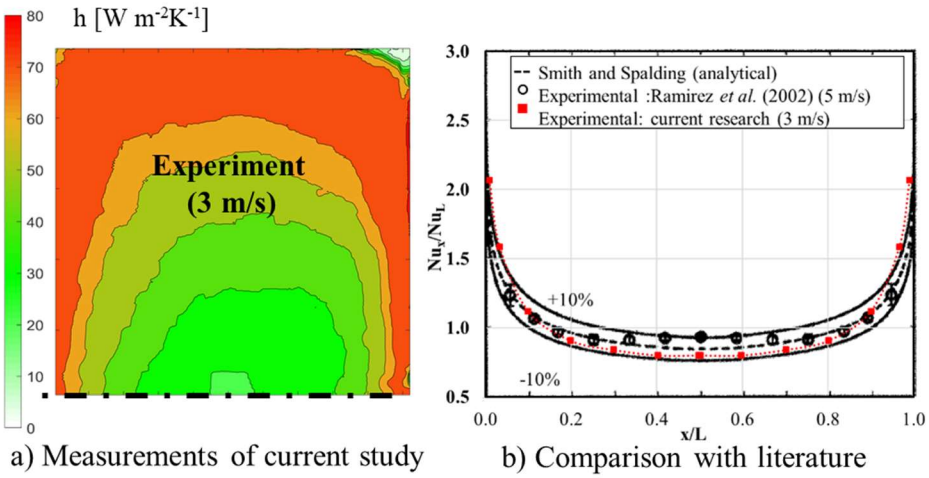

Figure 7: Local HTCs of Hiemenz flow, (a) Measures of the current study, (b) Comparison with literature

Moreover, laminar flow over a flat plate has a well-accepted analytical solution (Blasius solution), the accuracy of the CTC method has been evaluated under this classical flow condition by Che and Elbel (2019). The measurements of span-averaged HTCs compared to the Blasius solution at the same condition. The errors at the vicinity of edges are within 15% and within 5% at the inner locations of the sample compared to the Blasius solution. Local HTCs of external laminar flow over cylinders of different diameters have been evaluated and compared with results in the literature. The measurements of the current study agree well with the measurements of Krall and Eckert (1973) and the analytical solution from Goland (1950) before the separation point on the cylinder.

5. EXPERIMENTAL RESULTS ON FAN BLADES

5.1 Two-Dimensional Tangential Velocity Distribution on Blade Surfaces

The geometric parameters of two fan samples that have been evaluated in current research are shown in Table 2. The geometric parameters of the two fan samples are very similar in respect to the number of blades, blade diameter, hub diameter, and chord length. However, the blade shapes of the two samples are very different. Moreover, the direction of rotation is opposite. The two samples have been set to rotate at the same speed for comparison. Tangential flow velocity distribution on both high-pressure and low-pressure side have been evaluated.

Table 2: Fan blade sample geometric parameters

Sample #1					
Parameter	**Units**	**value**	**Parameter**	**Units**	**value**
Tip radius	m	0.1969	Tip chord length	m	0.2794
Hub radius	m	0.0635	Tip stagger angle	°	38
Hub to tip ratio	-	0.32	Impeller speed	$r \cdot min^{-1}$	900
Number of blades	-	3	Other	-	Ribs on low pressure side
Sample #2					
Parameter	**Units**	**value**	**Parameter**	**Units**	**value**
Tip radius	m	0.2032	Tip chord length	m	0.2900
Hub radius	m	0.0635	Tip stagger angle	°	29
Hub to tip ratio	-	0.31	Impeller speed	$r \cdot min^{-1}$	900
Number of blades	-	3	Other	-	Dimples on low pressure side

Figures 8 show the color change images at a different time on the high and low-pressure sides of fan sample #1. By observation, the color change is faster at the leading edges, and then moving toward the trailing edge. It is worth mentioning that the mass transfer and color change will not happen if no ammonia is injected. Similar images of the high-pressure side and fan sample #2 have been obtained to obtain two-dimensional velocity distributions.

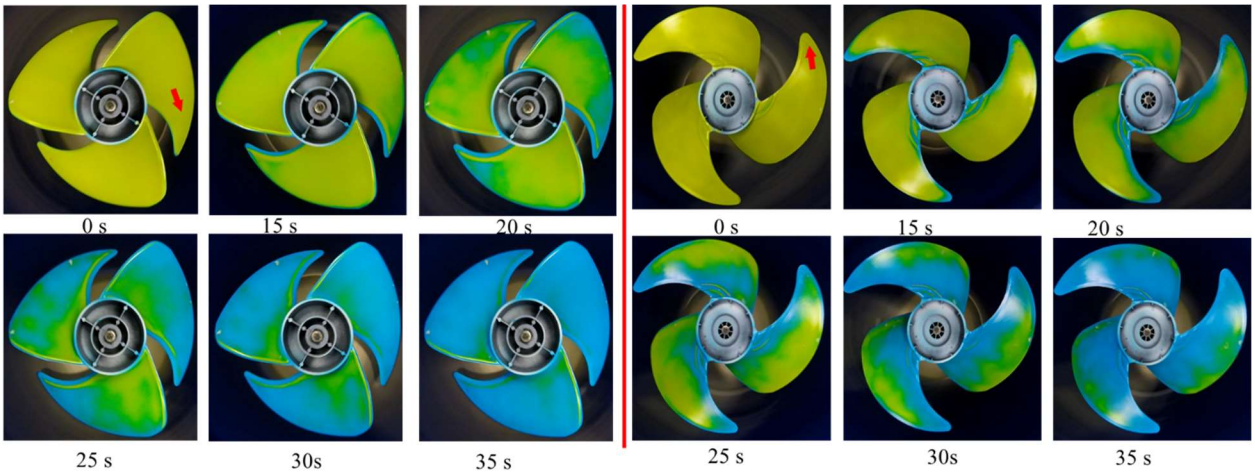

(a) High-pressure side of fan sample #1 (a) Low-pressure side of fan sample #1

Figure 8: Color change observation

The tangential flow velocity distributions on the blade surfaces are shown in Figures 9 and 10. For fan blade sample #1 which is shown in Figure 9, higher velocities are observed at the leading edge and decrease toward the trailing edge and hub area on the high-pressure side. For the low-pressure side, a similar trend is observed. Moreover, higher velocities are observed on the ribs because the airflow is interrupted by the rib structure. For blade sample #, the velocity distribution of the airflow is relatively uniform at both the high-pressure and low-pressure sides. Due to the symmetric blade arrangement, tangential airflow velocity distributions are similar on three blades.

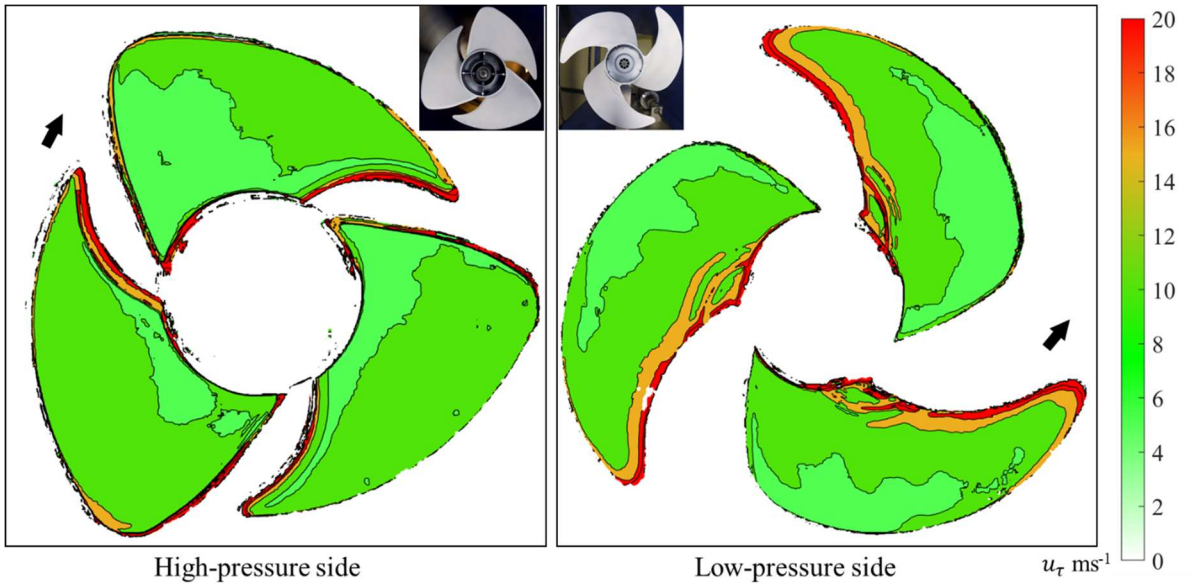

Figure 9: Two-dimensional tangential airflow velocity distribution on blade surface (sample #1)

The experimental results of blade sample #2 are shown in Figure 11. At the high-pressure side, higher velocities are observed at the leading and the trailing edge. Flow separation and reattachment are observed behind the tip of the blades due to their curved shape. By observation, the curved blade shape on the high-pressure side causes instability of the airflow. Moreover, vortexes at the trailing edge are anticipated due to the blade shape which shows higher velocity at this location. On the low-pressure side, the airflow velocities are much higher than on the high-pressure side due to the dimpled surface geometry. The dimples break the boundary layer, generate vortexes, and disturbance to the airflow. Therefore, for sample #2, a larger static pressure difference between the high-pressure and low-pressure sides is expected. Meanwhile, there might be a higher friction loss on the surface. However, according to Equations (4) and (9), intake flow velocity (U_i) need to be measured to obtain local wall shear stress (τ_w). To make a fair comparison of two fan blade samples, flow rate, static pressure, and power consumption need to be measured as well.

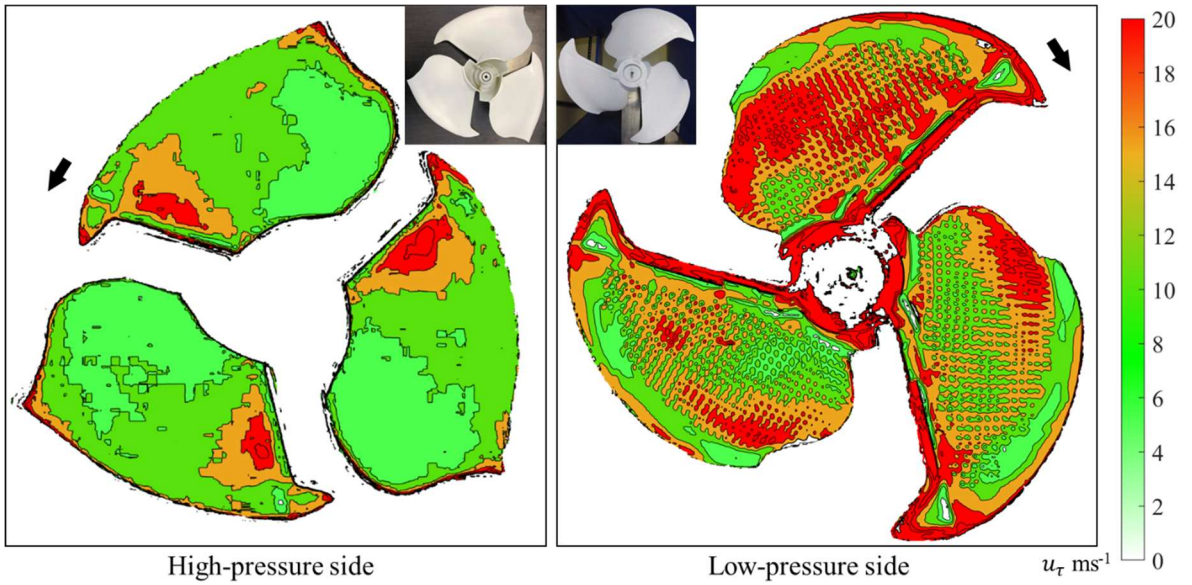

Figure 11: Two-dimensional tangential airflow velocity distribution on blade surface (sample #2)

6. CONCLUSION AND FUTURE WORK

The newly developed CTC method which has been validated and employed on local heat transfer measurements can be utilized to evaluate axial fans. To the authors' best knowledge, this is the first experimental result of two-dimensional velocity distributions at the boundary layer on the fan blade surfaces in the open literature. In the current research, the CTC method was employed to measure turbulent flow. From the preliminary results obtained in current research, the interaction between tangential flow velocity and blade surface geometry is observed. This new experimental method has been proved as a convenient and robust tool to compare different fan blades. By combing these local velocity measurements with global fan performance measurements, the best design options can be identified with better confidence. Moreover, it can be used as a reliable tool to verify and improve CFD models. There are some advantages of this method. It is promising to be utilized to investigate opportunities to improve efficiency and reduce the noise of the fan system.

1) Non-intrusive velocity measurements of rotating fan blades
2) Obtain high-resolution two-dimensional velocity distribution on large surface areas
3) The simple experimental procedure, low cost on both sample preparation and experimental setup, and robust

Due to the complexity of fan blade geometry, the two-dimensional image has caused some information loss in the axial direction. Therefore, three-dimensional image acquisition and processing will be explored in future study. Meanwhile, the experimental setups will be upgraded by considering tip clearance and fan shroud. Therefore, the whole fan assembly can be evaluated. The global measurements such as total flow rate, power input, static pressure, and sound pressure should also be obtained to investigate the relation between the local velocity distribution on the blade surface. Moreover, the fluid velocity at the external of the boundary layer on the surface of the whole fan assembly including blades, hub, the shroud can be evaluated by applying coatings on all surfaces of interest. Therefore, a comprehensive fan system evaluation can be obtained.

NOMENCLATURE

Symbols and Abbreviations

A	Total surface area (m^2)	T	Temperature (K)
AMS 71	coating material designation	t	Time (s)
CTC	Coating, tracer, and color change (-)	u	Flow velocity in x direction ($m\ s^{-1}$)
c_f	Friction factor (-)	U	Free stream flow velocity ($m\ s^{-1}$)
C	Concentration ($kg\ m^{-3}$)	U_i	Intake flow velocity ($m\ s^{-1}$)
D	Diffusion coefficient ($m^2\ s^{-1}$)	α	Thermal diffusivity ($m^2\ s^{-1}$)
HTC	Heat transfer coefficient ($W\ m^{-2}\ K^{-1}$)	τ	Wall shear stress (Pa)
h	Heat transfer coefficient ($W\ m^{-2}\ K^{-1}$)	ϵ	Ratio of color change (-)
h_m	Mass transfer coefficient ($kg\ m^{-2}\ s^{-1}$)	ϵ_H	Thermal eddy diffusivity ($m^2\ s^{-1}$)
k_f	Thermal conductivity of fluid ($W\ m^{-1}\ K^{-1}$)	ϵ_M	Momentum eddy diffusivity ($m^2\ s^{-1}$)
L_c	Chord length (m)	ϵ_m	Mass eddy diffusivity ($m^2\ s^{-1}$)
M	Mass of ammonia absorption (g)	μ	Dynamic viscosity of air ($N\ s\ m^{-2}$)
Nu	Local Nusselt number (-)	ν	Kinetic viscosity of air($m^2\ s^{-1}$)
P	Pressure (Pa)	Δ	Difference (-)
PIV	Particle image velocimetry (-)	θ	Cylinder angle (deg)
Pr	Prandtl number (-)	subscripts	
ppm	Concentration (parts-per-million)	loc	Local (-)
Re	Reynold number (-)	max	Maximum (-)
RH	Relative Humidity (%)	tot	Total (-)
RPM	Rotation per minute ($r\ min^{-1}$)	v	Volumetric (-)
S	Color change factor (-)	w	Wall (-)
Sc	Schmidt number (-)	∞	Free stream of the fluid
St	Heat transfer Stanton number (-)		
St_m	Mass transfer Stanton number (-)		

REFERENCES

Fukano, T., Kodama, Y., & Takamatsu, Y. (1977). Noise generated by low pressure axial flow fans, II: Effects of number of blades, chord length and camber of blade. *Journal of Sound and Vibration*, 50(1), 75-88.

Wallis, R. A. (1961). Axial Flow Fans: Design and Practice. New York. Academic Press.

Yang, L., Hua, O., & Zhao-Hui, D. (2007). Optimization design and experimental study of low-pressure axial fan with forward-skewed blades. *International Journal of Rotating Machinery*.

Jung, J. H., & Joo, W. G. (2019). The effect of the entrance hub geometry on the efficiency in an axial flow fan. *International Journal of Refrigeration*, 101, 90-97.

Wang, W., Li, S., Zeng, L., Liu, L., & Li, X. (2011). Numerical Predictions of the Broadband Turbulent Noise for Axial Flow Cooling Fans. *HVAC&R Research*, 17(5), 781-797.

Che, M., & Elbel, S. (2019). An experimental method to quantify local air-side heat transfer coefficient through mass transfer measurements utilizing color change coatings. International Journal of Heat and Mass Transfer, 144, 118624.

Che, M., & Elbel, S. (2021). Experimental Evaluation of Local Air-Side Heat Transfer Coefficient on Single Fins. 18th International Refrigeration and Air Conditioning Conference at Purdue, Paper 2176.

Bejan, A. (1995). Convection Heat Transfer, second edition., Wiley, New York.

Tien, K. K., & Sparrow, E. M. (1979). Local heat transfer and fluid flow characteristics for airflow oblique or normal to a square plate. *International Journal of Heat and Mass Transfer*, 22(3), 349-360.

Ramirez, O. M., Constantinou, M. C., Gomez, J. D., Whittaker, A. S., & Chrysostomou, C. Z. (2002). Evaluation of simplified methods of analysis of yielding structures with damping systems. *Earthquake Spectra*, 18(3), 501-530.

Krall, K. M., & Eckert, E. R. G. (1973). Local heat transfer around a cylinder at low Reynolds number. *Journal of Heat Transfer*, 95(2), 273-275

Leonard Goland. (1950). A theoretical investigation of heat transfer in the laminar flow regions of airfoils. *Journal of the Aeronautical Sciences*, 17(7), 436-440.

ACKNOWLEDGEMENTS

The authors would like to thank the member companies of the Air Conditioning and Refrigeration Center at the University of Illinois at Urbana-Champaign for their financial and technical support. The authors would like to thank Creative Thermal Solutions, Inc. (CTS) for providing technical support and equipment. The coating solutions are developed by Serionix, Inc., located in Champaign, IL.